

# Real time HR–MAS NMR: application in reaction optimization, mechanism elucidation and kinetic analysis for heterogeneous reagent catalyzed small molecule chemistry<sup>†</sup>

Abhijeet Deb Roy,<sup>a</sup> K. Jayalakshmi,<sup>c</sup> Somnath Dasgupta,<sup>b</sup> Raja Roy<sup>a,c,\*</sup> and Balaram Mukhopadhyay<sup>b</sup>



A novel application of *in situ* <sup>1</sup>H high-resolution magic angle spinning (HR–MAS) NMR technique for real-time monitoring of H<sub>2</sub>SO<sub>4</sub>-silica promoted formation of 2, 2-disubstituted quinoxalin-4(3H)-ones is reported. The detailed NMR spectroscopic data led to elucidation of the mechanism, reaction optimization, kinetics and quantitative analysis of the product accurately and efficiently. The translation of the optimized parameters obtained by <sup>1</sup>H HR–MAS NMR in the wet laboratory provided similar results. It is proposed that <sup>1</sup>H HR–MAS has a potential utility for optimization of various organic transformations in solid supported catalyzed reactions. Copyright © 2008 John Wiley & Sons, Ltd.

Supporting information may be found in the online version of this article.

**Keywords:** HR–MAS NMR; heterogeneous catalyst; kinetics; disubstituted quinoxalines

## Introduction

Magic angle sample spinning (MAS) is one of the cornerstones in high-resolution NMR of solid and semisolid materials.<sup>[1]</sup> High-resolution magic angle spinning (HR–MAS) NMR, initially developed in the late 1990s, has been used to characterize various biological samples and for the study of gene mutation and drug treatment in mammalian cells.<sup>[2]</sup> HR–MAS NMR spectroscopy evolved from solid-state NMR techniques is also being used as a method to analyze <sup>1</sup>H spectra of molecules attached to solid-phase synthetic resins.<sup>[3]</sup> It allows the analysis of materials that swell, become partially soluble, or form true solutions in a solvent even when some solids are still present.<sup>[4]</sup> In an HR–MAS experiment, a heterogeneous or multiphase sample is spun at a high speed (typically 3–5 kHz) around an axis oriented at an angle of 54.7° (the so-called magic angle) with respect to the direction of the static magnetic field. MAS averages out all the anisotropic magnetic interactions (including residual dipolar couplings, anisotropic chemical shifts, and bulk susceptibility effects) that are responsible for additional line broadening in heterogeneous samples and prevent the acquisition of well-resolved spectra under conventional liquid conditions. As a result, the MAS technique allows NMR spectra of heterogeneous systems characterized by line widths comparable to those of classic solution state NMR spectra. In recent years the application of HR–MAS NMR has not only gained unparalleled importance in the field of metabolomics<sup>[5]</sup> but has also become the single most significant, sensitive and nondestructive analytical method for obtaining detailed structure information of a compound covalently bound to a resin support.<sup>[6]</sup> It has also been used to monitor the progress of the solid-phase reaction and to determine the chemical structure of a compound bound on a single bead. Owing to the unmatched

quantum of information that HR–MAS NMR provides, it has now become one of the most widely used and recognized techniques in the fields of both chemistry and biology.<sup>[7]</sup>

The application of <sup>1</sup>H HR–MAS NMR in synthetic organic chemistry has mainly been restricted so far only to the area of solid phase organic synthesis (SPOS) for the quantification and step-by-step analysis of supported organic reactions. The growing interest for the use of solid supported catalyst for various organic transformations in a greener and safer environment encouraged us to evaluate the application of the above technique to unveil the real-time mechanistic insight of these reactions.<sup>[8]</sup> The major problem associated with the use of solution phase NMR technique for real-time heterogeneous reactions is the peak broadening because of the presence of solids and chemical shift anisotropy created by the catalyst during the experiment followed by loss of time because of manual off-axis shimming for the suppression of spinning side bands. In nonspinning mode the solid catalyst settles down quickly, slows down the

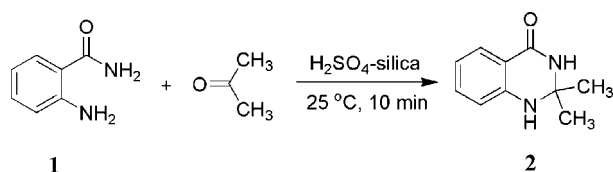
\* Correspondence to: Raja Roy, Sophisticated Analytical Instrument Facility, Central Drug Research Institute, Chatter Manzil Palace, Lucknow, India 226 001, India. E-mail: rajaroy\_cdri@yahoo.com

† CDRI Communication No. 6956.

a Sophisticated Analytical Instrument Facility, Central Drug Research Institute, Chatter Manzil Palace, Lucknow, India 226 001, India

b Medicinal and Process Chemistry Division, and Central Drug Research Institute, Chatter Manzil Palace, Lucknow, India 226 001, India

c Centre of Biomedical Magnetic Resonance, Sanjay Gandhi Post Graduate Institute of Medical Sciences, Lucknow, India



**Scheme 1.** H<sub>2</sub>SO<sub>4</sub>-silica promoted reaction of anthranilamide with acetone.

reaction and does not allow mimicking the reaction as carried out in the wet laboratory. In both spinning and nonspinning situations in solution state NMR, isotropic mixing of the reaction mixture cannot be induced in a reaction having heterogeneous catalyst. This unavoidable drawback as we experienced in our endeavors has drawn our attention toward real-time HR-MAS NMR involving a heterogeneous catalyzed reaction. To establish the utility of the technique, we opted for an otherwise simple reaction so that the clarity of the outcome enables us to justify our exploration. Formation of the privileged class of 2,2-di-substituted quinazolin-4(3H)-ones from anthranilamide and various ketones is an important and well-reported reaction using various Lewis/Bronsted acids.<sup>[9]</sup> We observed that H<sub>2</sub>SO<sub>4</sub> immobilized on silica is also capable of doing this transformation smartly leading to excellent yield of the target in a practical time frame and a much greener way. Thus, this reaction was chosen for our study of real-time HR-MAS experiment monitoring. Here, we report a novel application of HR-MAS NMR in reaction optimization, mechanism elucidation and kinetic analysis for heterogeneous reagent catalyzed synthesis of 2,2-di-substituted quinazolin-4(3H)-ones.

## Results and Discussion

### NMR analysis

The reaction was initially standardized using the commercially available anthranilamide (**1**, 1 mmol) and acetone (1 ml) in the presence of H<sub>2</sub>SO<sub>4</sub> silica as the heterogeneous catalyst (10 mg) in 10 ml of dry methanol. It showed complete conversion of the starting material to a faster running component on TLC within 10 min at room temperature (Scheme 1). The compound was obtained in almost quantitative yield after filtration and evaporation of the solvent and was confirmed to be the desired 2,2-di-methyl quinazolin-4(3H)-one (**2**) by NMR spectroscopy and mass spectrometry. No traces of the starting material or any other byproducts were detected. To get an insight into the mechanism of this quinazolinone formation, the reaction was monitored by real-time NMR measurements in HR-MAS probe using 50  $\mu$ l of the total reaction mixture under stoichiometric conditions (0.11 mmol of anthranilamide, 10  $\mu$ l of acetone and 1 mg of catalyst in 40  $\mu$ l of methanol-*d*<sub>4</sub>). The recording of the HR-MAS NMR spectra were carried out as soon as the spinning speed was achieved (4.0 kHz) without any further shimming. Hence, the time between sample preparation and recording of the NMR spectra was approximately between 1 and 2 min. Similar, real-time NMR measurements under automation was also performed on 5-mm solution state probe head in spinning as well as in nonspinning mode, but no meaningful observation could be deciphered from the recorded data because of initial inhomogeneity of the sample followed by the nonisotropic mixing of the catalyst leading to incomplete reaction.

The NMR stack plots (Fig. 1) and their zoomed portions (Fig. 1(a–e)) clearly indicate the formation of the intermediate

Schiff base (Fig. 1(a)) as the emergence of the dimethyl signal at 1.25 ppm in the beginning, which subsequently diminishes during the course of the reaction. The completion of the reaction was identified by the emergence of the dimethyl resonance at 1.45 ppm (Fig. 1(b)) and the signals of the product (Fig. 1(c)) with nearly complete disappearance of the acetone signal (Fig. 1(d)), which showed more than 95% of conversion of the starting material as shown in the buildup curve of the reaction (Fig. 2).

For the synthesis of 2,2-di-substituted quinazolin-4(3H)-ones using a heterogeneous acid catalyst two plausible pathways can be drawn (path A and path B, Fig. 3). Out of these two mechanisms the former was discarded since from the second spectrum onwards the dimethyl signal of the acetone reactant showed a distinct splitting that not only revealed the presence of two forms of acetone in the system (Fig. 1(d)), protonated and the nonprotonated acetone, but also indicated the initiation of the reaction by the acid catalyst. The splitting of the acetone signal then disappeared with time indicating complete protonation of the entire acetone reactant. In another experiment, no change was observed in the anthranilamide spectrum in the absence of the acid catalyst, which indicated that the involvement of the acid source for the protonation of the ketone was the initial step that drove the reaction in the forward direction. This was further reinstated by the initial splitting of the HOD (partially deuterated water present in deuterated methanol) signal (Fig. 1(e)) in its protonated and nonprotonated forms owing to involvement of the acid catalyst. Concomitantly, appearance of reaction intermediates signals followed by the equilibrium shift to the formation of hydrazone with coherent appearance of the final product, 2,2-disubstituted quinazolinone (**2**) was clearly visible from the initial stage of monitoring. Whereas, the fully protonated HOD signal appears as a singlet at the later time of the reaction, hence the reaction proceeds via path B (Fig. 3).

Identical experiments were then performed using the higher alkyl ketone analogue of ethyl propyl ketone and identical results were obtained at room temperature. In this case, the time taken for the reaction to complete was longer than the previous one and the reaction was rather slow which provided us the better overview of the initial process. The entire changes initially observed in this case were in the ketone resonances rather than in the anthranilamide resonances, which were again due to the protonation of the ketone moiety first, supporting the second mechanistic pathway and the final product was found to be 2-ethyl-2-propyl-2,3-dihydro-1H-quinazolin-4-one (**3**) (Scheme 2).

Successful execution of the real-time HR-MAS technique for the reaction monitoring and evaluation of the mechanistic pathway with alkyl ketones prompted us to investigate the reaction involving an aromatic ketone along with its kinetic analysis in order to provide quantitative results for the reaction. Thus stoichiometric amount of acetophenone was reacted with anthranilamide in methanol using H<sub>2</sub>SO<sub>4</sub> silica. The standardization of the reaction was carried out in the HR-MAS rotor itself using *in situ* HR-MAS experiments followed by the synthesis of the compound in the wet lab. In the beginning, the reaction was performed at room temperature using same amount of catalyst as used in the acetone reaction but the reaction did not proceed for 3 h and only 20–25% of the final product could be identified even after 8 h. Therefore, in order to achieve the desired result while keeping same amount of catalyst, the temperature of the reaction mixture was standardized with an increment of 10 °C at a time and the optimum reaction temperature was found to be at 50 °C. In the next set of experiments, the reaction was monitored at 50 °C and the

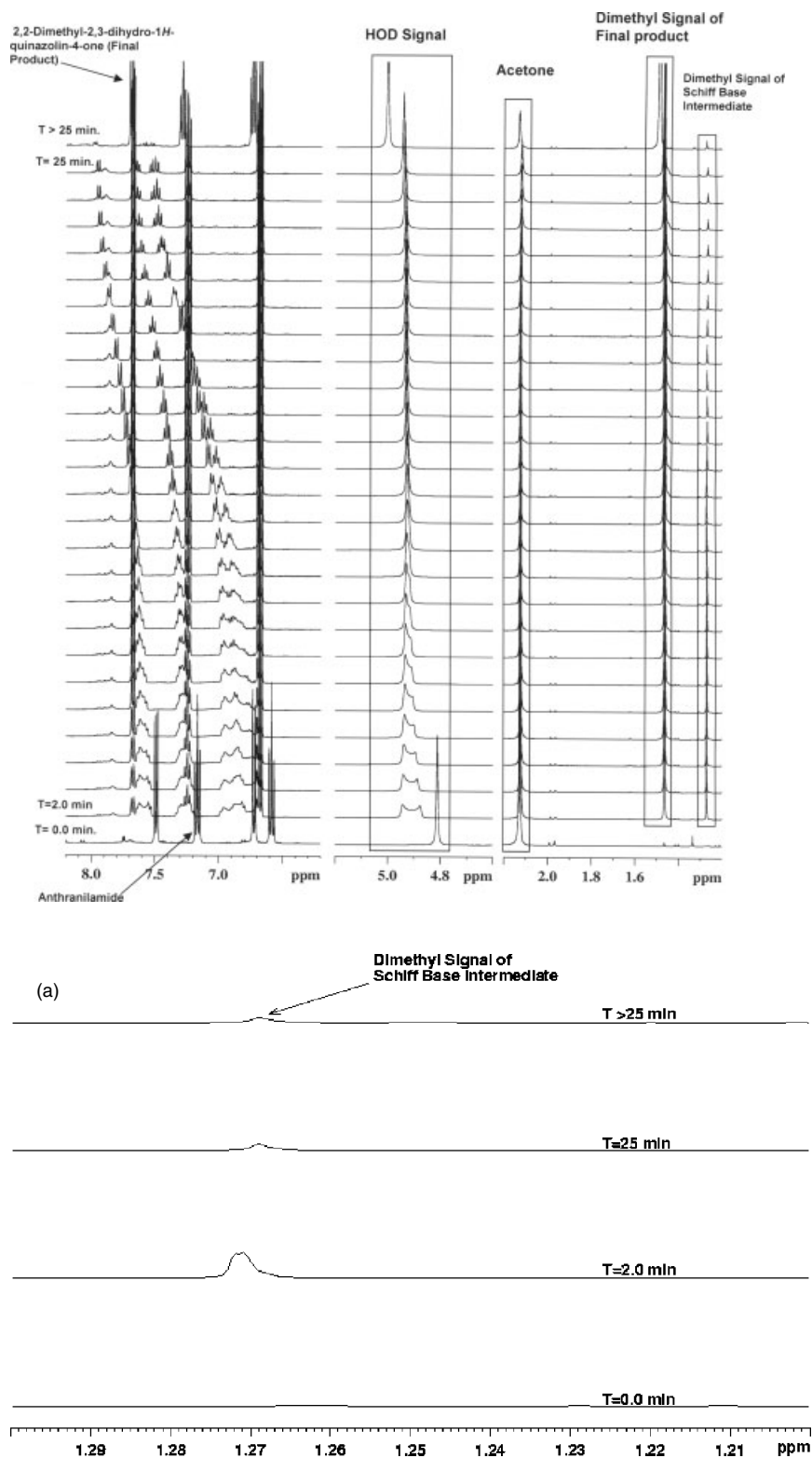


**Figure 1.** Represents a stack plot of 27 NMR spectra out of 40 NMR data recorded at 4.0 kHz spinning rate under automation in 25 min time with eight number of scans in each experiment. The first NMR spectrum represents anthranilamide and acetone resonances in the mixture prior to the addition of the catalyst followed by real-time NMR spectra of the reaction with the catalyst until the completion of the reaction. The series of spectra provided the snapshots of the mechanistic pathways of the reaction. The last spectrum represents the final product of the same sample after 25 min. (a) Expanded region (1.30–1.20 ppm) of the stack plot of four NMR spectra of 0.0, 2.0, 25.0 and >25.0 min from Fig. 1. (b) Expanded region (1.60–1.40 ppm) of the stack plot of four NMR spectra of 0.0, 2.0, 25.0 and >25.0 min from Fig. 1. (c) Expanded region (8.50–5.50 ppm) of the stack plot of four NMR spectra of 0.0, 2.0, 25.0 and >25.0 min from Fig. 1. (d) Expanded region (2.20–2.00 ppm) of the stack plot of four NMR spectra of 0.0, 2.0, 25.0 and >25.0 min from Fig. 1. (e) Expanded region (5.10–4.65 ppm) of the stack plot of four NMR spectra of 0.0, 2.0, 25.0 and >25.0 min from Fig. 1.

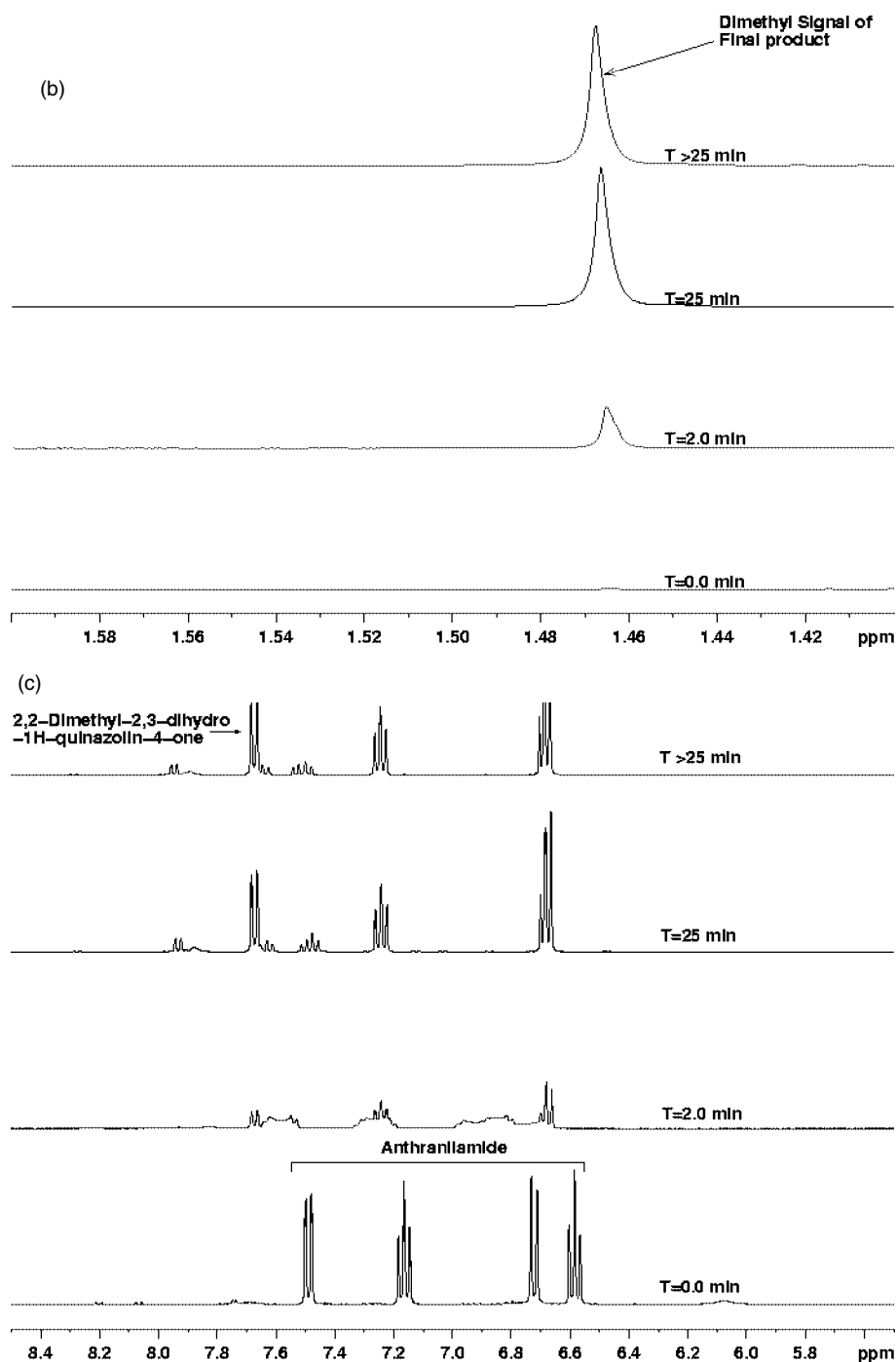


Figure 1. (Continued).

NMR spectra (Fig. 4) showed an immediate emergence of methyl signal of the quinazolinone at 1.75 ppm, which subsequently increased with time and was characterized as 2-methyl-2-phenyl-2,3-dihydro-1H-quinazolin-4-one (**4**) (Scheme 3).

### Kinetic and analysis

The rate constant of the reaction between anthranilamide and acetophenone was then determined using second-order rate equation,  $a = b$  and  $[A] \neq [B]$ .<sup>[10]</sup>

$$k_A = \frac{2.303}{t(a_0 - b_0)} \log_{10} \left[ \frac{b_0(a_0 - x)}{a_0(b_0 - x)} \right] \text{ dm}^3 \text{ mol}^{-1} \text{ s}^{-1}$$

where  $a_0$  and  $b_0$  are the initial concentrations of the acetophenone and anthranilamide, respectively and  $x$  is the amount of the product formed at time  $t$ .

$a_0 - x$  and  $b_0 - x$  are the concentration of acetophenone and anthranilamide at time  $t$ .

Because of the absence of any standard reference in the reaction, change in concentration of the reactants and the product with respect to time was calculated using the integral values of all

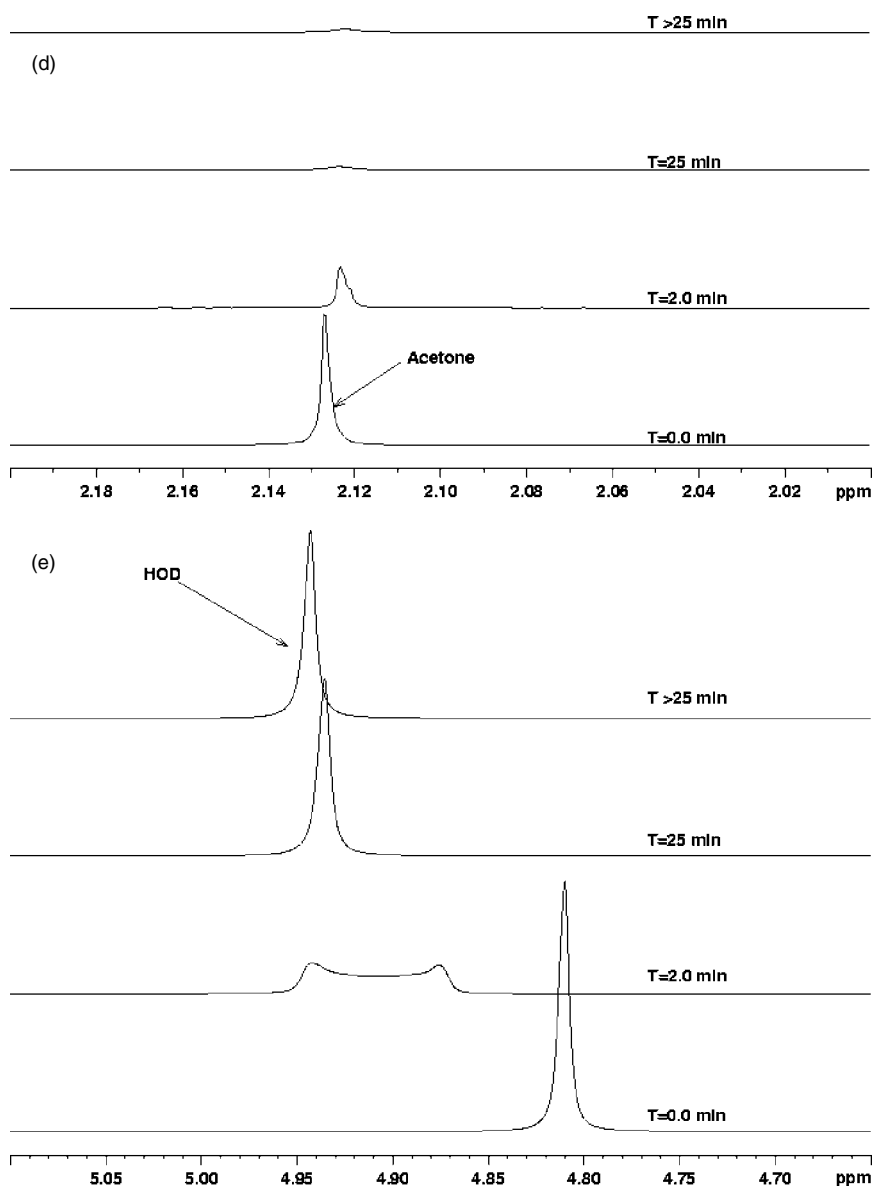


Figure 1. (Continued).

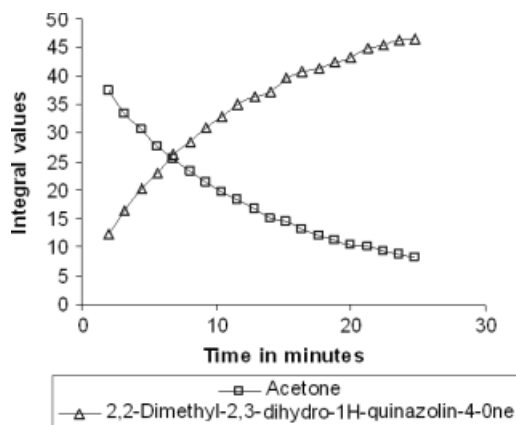
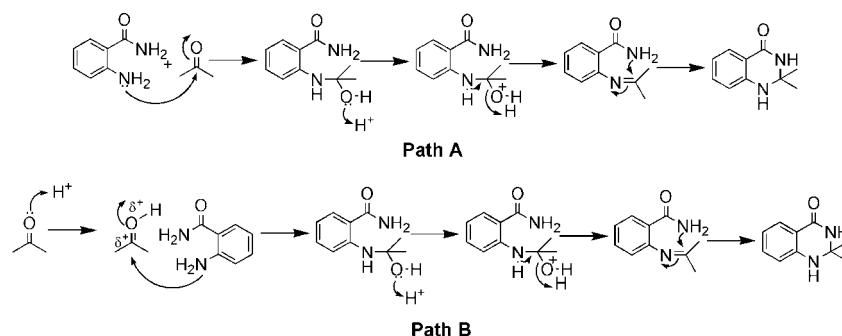


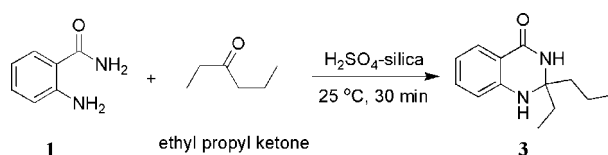
Figure 2. Buildup curve of the product 2,2-dimethyl-2,3-dihydro-1H-quinazolin-4-one along with the decay curve of the reactant, acetone.

the experiments by integrating the anthranilamide resonance at 6.72 ppm, acetophenone signal at 2.41 ppm, and the product signal at 1.75 ppm. In this reaction almost 85% conversion was clearly observed by simple visualization of the real-time HR-MAS spectrum after 5 h. The percentage of the product formed was found to be 83.99% by theoretical calculations and the results were found to be similar when the reaction was carried out in the wet lab in which the reaction provided 87% crude product in 4 h time.

Subsequently the rate constant for the same reaction was calculated by plotting<sup>[10]</sup>  $\log[b_0(a_0 - x)/a_0(b_0 - x)]$  versus time ( $t$ ) in seconds. Though the plotted curve is discontinuous, the reaction mainly follows second-order reaction mechanism with the rate constant of  $109 \times 10^{-6} \text{ dm}^3 \text{ mol}^{-1} \text{ s}^{-1}$  as shown in Fig. 5. Similarly, calculation of the rate constant at the middle of the reaction showed it to be  $108 \times 10^{-6} \text{ dm}^3 \text{ mol}^{-1} \text{ s}^{-1}$  which was similar for the whole reaction. This indicates that the reaction mainly follows second-order kinetics.



**Figure 3.** Plausible mechanisms of the acid-catalyzed quinazolinone formation.



**Scheme 2.**  $\text{H}_2\text{SO}_4$ -silica promoted reaction of anthranilamide with ethyl propyl ketone.

Moreover, the reaction of anthranilamide with acetophenone was also carried out at room temperature using double the amount of catalyst, which expectedly showed the protonation of the ketone along with the emergence of Schiff base methyl signal, but the reaction did not proceed further at this temperature. Thus, on the basis of these results it was concluded that for the reaction to move in forward direction from the Schiff base intermediate to the final cyclized product a much higher temperature is required.

## Conclusion

In summary, we have shown that the progress of a heterogeneous reagent catalyzed reaction could be monitored using real-time HR-MAS NMR spectroscopy. These observations open a new avenue of  $^1\text{H}$  HR-MAS real-time monitoring of the reaction. The results not only provided information about the completion of the reaction but it also afforded the product yield, which could be quantified using this technique. In addition, the monitoring provided us an insight into the reaction, allowing a simple evaluation of the reaction mechanism. This information is also valuable when trying to optimize reaction conditions.

## Experimental Section

### General consideration

All the products were characterized by  $^1\text{H}$ ,  $^{13}\text{C}$ , DEPT90, DEPT135, two-dimensional heteronuclear single quantum coherence (HSQC), heteronuclear multiple bond correlation (HMBC) spectroscopy, Fast Atom Bombardment Mass Spectrometry (FAB-MS). All the chemicals used in the study were purchased from Sigma Aldrich.

The NMR spectra were recorded at 303 K using a Bruker Avance 400 MHz and Avance DRX 300 MHz FT-NMR spectrometer equipped with a 5-mm multinuclear inverse probe head with z-shielded gradient. Time dependent HR-MAS  $^1\text{H}$  NMR experiments were recorded with 400 MHz FT-NMR spectrometer using 4 mm

$^1\text{H}/^{13}\text{C}$  HR-MAS dual probehead equipped with magic angle gradient in  $\text{CD}_3\text{OD}$  in a two-dimensional format. Chemical shifts are given on the ppm scale and are referenced to the TMS at 0.00 ppm for proton and for  $^{13}\text{C}$  NMR spectra. In the one-dimensional measurements ( $^1\text{H}$ ,  $^{13}\text{C}$  and DEPT) 32 K data points were used for the FID. The pulse programs of the following 2D experiments were taken from the Bruker software library and the parameters were as follows.

300/75 MHz gradient HSQC spectra: relaxation delay  $d_1 = 2$  s; evolution delay  $d_2 = 3.44$  ms;  $90^\circ$  pulse,  $6.85 \mu\text{s}$  for  $^1\text{H}$ ,  $10 \mu\text{s}$  for  $^{13}\text{C}$  hard pulses at  $-3.0$  dB and  $60 \mu\text{s}$  for  $^{13}\text{C}$  Globally optimized Alternating phases of Rectangular Pulses (GARP) decoupling with gradient ratio GPZ1 : GPZ2 : GPZ3 = 50 : 30 : 40.1; 1024 data points in  $t_2$ ; spectral width 9.0 ppm in F2 and 160 ppm in F1; number of scans 32; 256 experiments in  $t_1$ ; linear prediction to 512; zero filling up to 1 K and apodization with sine bell in both dimensions prior to double Fourier transformation.

300/75 MHz gradient HMBC spectra: relaxation delay  $d_1 = 2$  s; delay of the low-pass J-filter  $d_2 = 3.44$  ms; delay for evolution of long-range coupling  $d_6 = 71$  ms with gradient ratio same as HSQC; 2048 data points in  $t_2$ ; spectral width 11.0 ppm in F2 and 240 ppm in F1; number of scans 52; 256 experiments in  $t_1$ ; linear prediction to 512; zero filling up to 2 K and apodization with  $90^\circ$  shifted square sine bell in F1 dimension and sine bell in F2 dimension prior to double Fourier transformation.

### General procedure for the synthesis of 2,2-disubstituted quinazolinone

To a solution of anthranilamide (200 mg, 1.5 mmol) and ketone (1.5 mmol) in dry methanol (10 ml) was added  $\text{H}_2\text{SO}_4$  silica (20 mg) and the mixture was stirred at the required temperature until TLC (1 : 1 *n*-hexane-ethyl acetate) showed complete conversion of the starting material. The mixture was filtered through Celite and the solvents were evaporated under reduced pressure. Compounds thus obtained were analyzed by NMR spectroscopy and mass spectrometry.

### General procedure for the $^1\text{H}$ HR-MAS NMR analysis

To a solution of anthranilamide (10 mg, 0.11 mmol) and ketone (1.5 mmol,  $10 \mu\text{l}$  in case of acetone) in deuterated methanol ( $40 \mu\text{l}$ ) was added  $\text{H}_2\text{SO}_4$  silica (1 mg) in a  $50 \mu\text{l}$  4 mm HR-MAS rotor and the rotor was sealed by spacer and screw cap. The HR-MAS rotor was then directly inserted in the prior shimmed and tuned 4 mm  $^1\text{H}/^{13}\text{C}$  HR-MAS dual probe. As soon as the spinning speed (4.0 kHz) was achieved, recording of the NMR data was carried out without further shimming of the probe for given time.

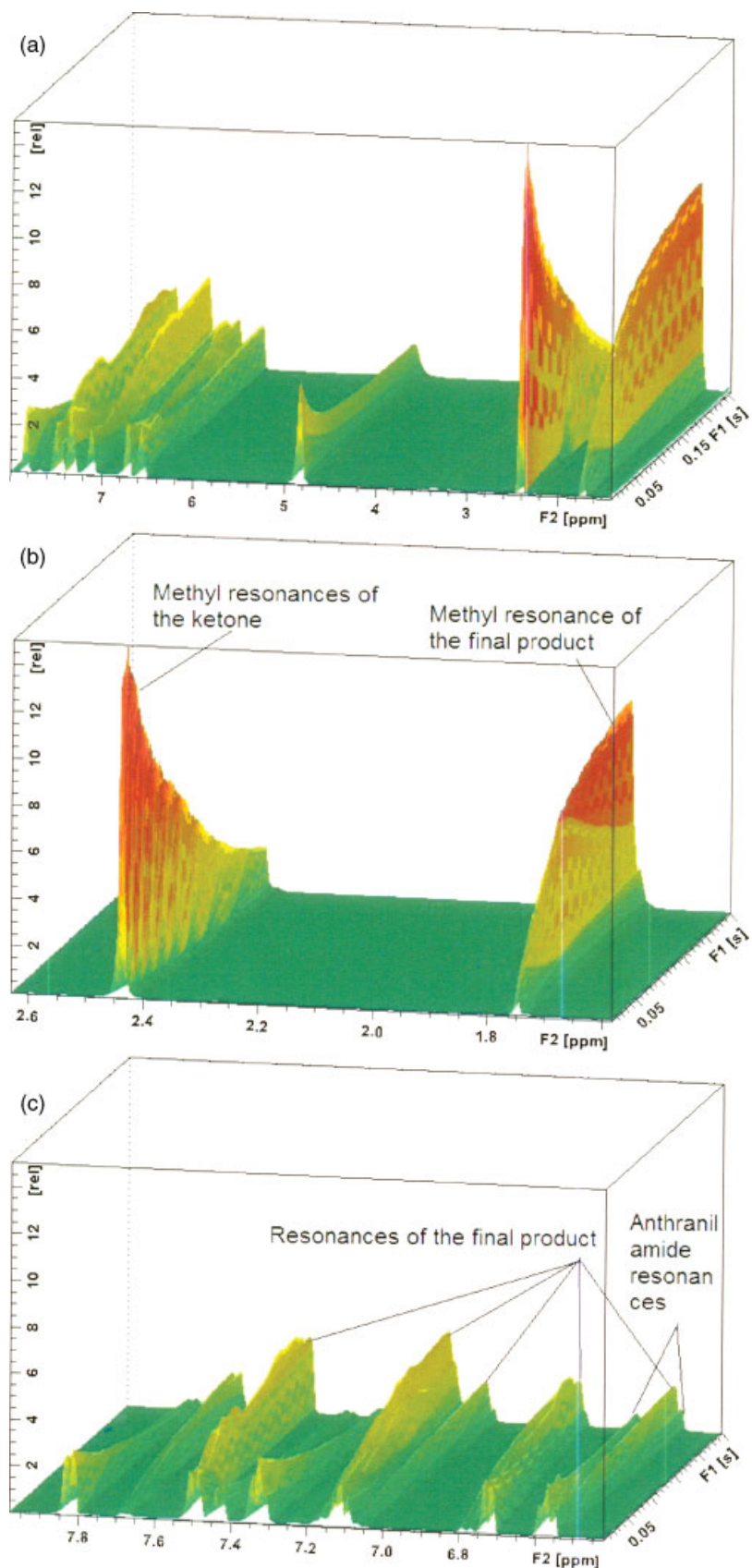
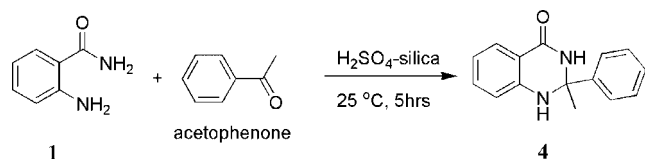


**Figure 4.** One-dimensional stack plot of *in situ*  $^1\text{H}$  NMR experiments with anthranilamide and acetophenone in methanol- $d_4$  in the presence of stoichiometric amount of  $\text{H}_2\text{SO}_4$  immobilized on silica. (a) Full spectrum; (b) and (c) expanded region.



**Scheme 3.** H<sub>2</sub>SO<sub>4</sub>-silica promoted reaction of anthranilamide with acetophenone.

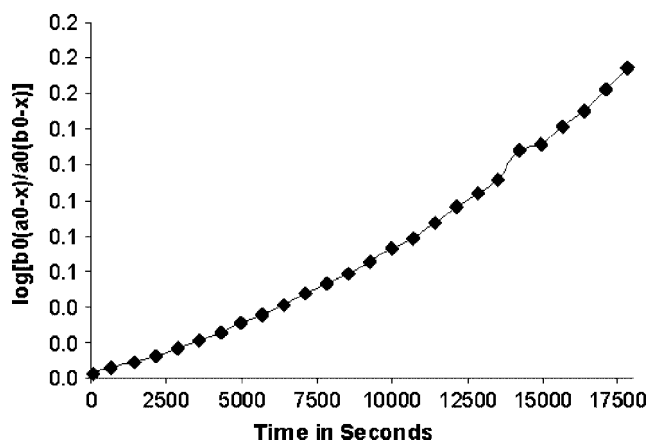


**Figure 5.** Plot of  $\log[b_0(a_0 - x)/a_0(b_0 - x)]$  versus time for the reaction between anthranilamide and acetophenone.

#### NMR analysis carried out 4.2.2. 2,2-dimethyl-2,3-dihydro-1H-quinazolin-4-one. (2)

251 mg (97% yield), <sup>1</sup>H NMR (CDCl<sub>3</sub>, 300 MHz)  $\delta$  = 1.56 (s, 6H, 2x-CH<sub>3</sub>), 4.24 (brs, 1H, -NH), 6.62 (d,  $J$  = 8.1 Hz, 1H, -ArH), 6.75 (brs(o), 1H, -NH), 6.81 (t(o),  $J$  = 7.5 Hz, 1H, ArH), 7.29 (t,  $J$  = 8.1 Hz, 1H, ArH), 7.88 (d,  $J$  = 7.8 Hz, 2H, ArH): <sup>13</sup>C NMR (CDCl<sub>3</sub>, 75 MHz)  $\delta$  = 29.6, 67.6, 114.6, 118.6, 128.3, 133.8, 145.9, 164.4. HRMS calcd. For C<sub>10</sub>H<sub>12</sub>N<sub>2</sub>NaO (M + Na): 199.0847; found:  $m/z$  199.0845.

#### 2-Ethyl-2-propyl-2,3-dihydro-1H-quinazolin-4-one (3)

311 mg (97% yield), <sup>1</sup>H NMR (CDCl<sub>3</sub>, 300 MHz)  $\delta$  = 0.89 (t(o),  $J$  = 7.5 Hz, 3H, -CH<sub>3</sub>), 0.95 (t(o),  $J$  = 7.2 Hz, 3H, -CH<sub>3</sub>), 1.43 (m, 2H, -CH<sub>2</sub>), 1.75 (m, 4H, 2x-CH<sub>2</sub>), 4.24 (s, 1H, -ArNH), 6.59 (d,  $J$  = 8.1 Hz, 1H, ArH), 6.73 (t,  $J$  = 7.5 Hz, 1H, ArH), 6.84 (brs, 1H, -CONH), 7.24 (t,  $J$  = 7.2 Hz, 1H, ArH), 7.83 (d,  $J$  = 7.5 Hz, 1H, ArH): <sup>13</sup>C NMR (CDCl<sub>3</sub>, 75 MHz)  $\delta$  = 7.8, 14.1, 16.7, 33.3, 42.6, 72.3, 114.0, 117.8, 128.1, 133.8, 146.4, 164.6. HRMS calcd. For C<sub>13</sub>H<sub>18</sub>N<sub>2</sub>NaO (M + Na): 241.1317; found:  $m/z$  241.1318.

#### 2-Methyl-2-phenyl-2,3-dihydro-1H-quinazolin-4-one (4)

325 mg (93% yield), <sup>1</sup>H NMR (CDCl<sub>3</sub> + DMSO-*d*<sub>6</sub>, 300 MHz)  $\delta$  = 1.80 (s, 3H, -CH<sub>3</sub>), 5.48 (brs, 1H, ArNH), 6.65–6.71 (m, 2H, ArH), 7.18–7.27 (m, 5H, ArH), 7.48 (d,  $J$  = 7.5 Hz, 2H, ArH), 7.74 (d,  $J$  = 7.5 Hz, 1H, ArH): <sup>13</sup>C NMR (CDCl<sub>3</sub> + DMSO-*d*<sub>6</sub>, 75 MHz)  $\delta$  = 30.2, 70.7, 114.6, 115.2, 118.5, 125.2, 127.8, 128.1, 128.3, 133.7, 145.5, 146.1, 164.6. HRMS calcd. For C<sub>15</sub>H<sub>14</sub>N<sub>2</sub>NaO (M + Na): 261.1004; found:  $m/z$  261.1001.

#### Supporting information

Supporting information may be found in the online version of this article.

#### Acknowledgements

ADR and SD are thankful to CSIR and JK is thankful to DST, New Delhi for providing fellowship.

#### References

- [1] E. R. Andrew, R. G. Eades, *Discuss. Faraday Soc.* **1962**, 34, 38.
- [2] G. Lippens, R. Warrass, J. M. Wieruszkeski, P. Rousselot Pailley, G. Chessari, *Comb. Chem. High Throughput Screening* **2001**, 4, 333.
- [3] G. Lippens, M. Bourdonneau, C. Dhalluin, R. Warass, T. Richert, C. Seetharaman, C. Boutillon, M. Piotto, *Curr. Org. Chem.* **1999**, 3, 147.
- [4] H. Schröder, *Comb. Chem. High Throughput Screening* **2003**, 6, 741.
- [5] J. L. Griffin, M. Bollard, J. K. Nicholson, K. Bhakoo, *NMR Biomed.* **2002**, 15, 375.
- [6] (a) M. J. Shapiro, J. S. Gounarides, *Biotechnol. Bioeng.* **2001**, 71, 130; (b) P. A. Keifer, *J. Org. Chem.* **1996**, 61, 1558; (c) R. Warrass, G. Lippens, *J. Org. Chem.* **2000**, 65, 2946; (d) A. M. Sefler, S. W. Gerritz, *J. Comb. Chem.* **2000**, 2, 127; (e) P. Rousselot-Pailley, N. J. Ede, G. Lippens, *J. Comb. Chem.* **2001**, 3, 559; (f) R. Hany, D. Rentsch, B. Dhanpal, D. Obrecht, *J. Comb. Chem.* **2001**, 3, 85; (g) Y. F. Ng, J. C. Meillon, T. Ryan, A. P. Dominey, A. P. Davis, J. K. Sanders, *Angew. Chem. Int. Ed.* **2001**, 40, 1757; (h) G. Deshayes, K. Poelmans, I. Verbruggen, C. Camacho-Camacho, P. Deg, V. Pinoie, J. C. Martins, M. Piotto, M. Biesemans, R. Willem, P. Dubois, *Chem. Eur. J.* **2005**, 11, 4552.
- [7] (a) J. C. Martins, F. A. G. Mercier, A. Vandervelden, M. Biesemans, J. M. Wieruszkeski, E. Humpfer, R. Willem, G. Lippens, *Chem. Eur. J.* **2002**, 8, 3431; (b) R. Warrass, J. M. Wieruszkeski, C. Boutillon, G. Lippens, *J. Am. Chem. Soc.* **2000**, 122, 1789; (c) R. Jelinek, A. P. Valente, K. G. Valentine, S. J. Opella, *J. Magn. Reson.* **1997**, 125, 185; (d) J. Chin, A. Chen, M. J. Shapiro, *Magn. Reson. Chem.* **2000**, 38, 782; (e) E. M. Ratai, S. Pilkenton, M. R. Lentz, J. B. Greco, R. A. Fuller, J. P. Kim, J. L. He, L. L. Cheng, R. G. González, *NMR Biomed.* **2005**, 18, 242; (f) J. H. Chen, E. B. Sambol, P. DeCarolis, R. O'Connor, R. C. Geha, Y. V. Wu, S. Singer, *Magn. Reson. Med.* **2006**, 55, 1246.
- [8] (a) B. Das, K. R. Reddy, P. Thirupathi, *Tetrahedron Lett.* **2006**, 47, 5855; (b) B. Mukhopadhyay, D. A. Russell, R. A. Field, *Carbohydr. Res.* **2005**, 340, 1075; (c) A. K. Misra, P. Tiwari, G. Agnihotri, *Synthesis* **2005**, 2, 260; (d) A. Agarwal, S. Rani, Y. D. Vankar, *J. Org. Chem.* **2004**, 69, 6137; (e) B. Mukhopadhyay, *Tetrahedron Lett.* **2006**, 47, 4337; (f) V. K. Rajput, B. Mukhopadhyay, *Tetrahedron Lett.* **2006**, 47, 5939; (g) V. K. Rajput, B. Roy, B. Mukhopadhyay, *Tetrahedron Lett.* **2006**, 47, 6987; (h) A. K. Chakraborti, R. Gulhane, *Chem. Commun.* **2003**, 15, 1896.
- [9] (a) T. Asano, T. Yoshikawa, T. Usui, H. Yamamoto, Y. Yamamoto, Y. Uehara, H. Nakamura, *Bioorg. Med. Chem.* **2004**, 12, 3529; (b) D. Shi, C. Shi, J. Wang, L. Rong, Q. Zhuang, X. Wang, *J. Heterocycl. Chem.* **2005**, 42, 173; (c) D. Shi, J. Wang, L. Rong, Q. Zhuang, S. Tu, H. Hu, *J. Chem. Res., Synop.* **2003**, 10, 671; (d) D. Shi, L. Rong, J. Wang, Q. Zhuang, X. Wang, H. Hu, *Tetrahedron Lett.* **2003**, 44, 3199; (e) D. J. Connolly, D. Cusack, T. P. O'Sullivan, P. J. Guiry, *Tetrahedron* **2005**, 61, 10153.
- [10] K. J. Laidler, *Chemical Kinetics* (3rd edn), Pearson Education: Singapore, **2004**, p 22.